Thermal radiation transferred to the guided modes of optical interference coatings

Paul Rouquette, Claude Amra, Myriam Zerrad, Helene Krol

Research Article | Vol. 32, No. 7 / 25 Mar 2024 / Optics Express 12065
Optics EXPRESS

Thermal radiation transferred to the guided modes of optical interference coatings

P. ROUQUETTE,[1,*] C. AMRA,[2] M. ZERRAD,[2] AND H. KROL[3]

[1]Aix Marseille Univ, CNRS, CNES, Laboratoire d'Astrophysique de Marseille, Marseille, France
[2]Aix Marseille Univ, CNRS, Centrale Marseille, Institut Fresnel, Marseille, France
[3]CILAS, 600 avenue de La Roche Fourcade, Pôle Alpha-Sud, 13400 Aubagne, France
[*]paul.rouquette@lam.fr

Abstract: An electromagnetic model is developed to predict the thermal radiation which is trapped in a multilayer structure and transferred to its guided modes. The theory is based on the electromagnetic power supplied by the thermal currents given by the fluctuation-dissipation theorem. The source of the radiation is the ambient temperature or that caused by the optical absorption of the component subjected to spatio-temporal illumination. A numerical example is given for a multi-dielectric mirror at thermodynamic equilibrium. It is shown that the thermal radiation transferred to the guided modes of the multilayer can be much larger or lower than the radiation emerging in free space outside the component.

1. Introduction

Thermal radiation [1–4] is ubiquitous in many situations, and has applications in many fields such as defense, space and energy. This radiation may also play an essential role in optical interference coatings [5,6], both for energy balances and for identification. These multilayer filters absorb part of the incident light, and this absorption is transferred in the form of thermal radiation, conduction and convection. In the space sector in particular, most heat is transferred by radiation, and this highlights the need to have at disposal a tool for an accurate prediction of the thermal power radiated per wavelength and per unit solid angle in each direction in space.

In this context, a great deal of work [7–10] has been devoted to modelling thermal radiation in multilayer optical filters. Some use indirect methods, which have the advantage of simplicity, and consist of relating the emissivity of the component to its absorption using Kirchhoff's law [1,8,11]. Other studies use direct methods, which are more complex because they require Maxwell's equations to be solved in the presence of thermal currents given by the fluctuation-dissipation theorem [2–4,7–10]. The advantage of these direct methods is that they take a more detailed look at the energy balance associated with the thermal radiation process. For example, they make it possible to calculate the proportion of energy transferred to evanescent waves [5] that are likely to be decoupled. They also make it possible, and this is the main focus of this work, to have access to the details of the thermal radiation trapped in the multilayer. We talk here of the amount of radiation that is transferred to each of the guided modes of the interference structure, and propagates parallel to the interfaces of the component (see Fig. 1).

There is little information in the literature on an energy balance that would include the contribution of this trapped thermal radiation [12,13] in the modes of a multilayer. In this article, we present an electromagnetic model giving access to this balance. This theoretical tool makes it possible to accurately quantify the coupling efficiency in each mode of the component. Numerical results are given for a multi-dielectric mirror structure.

Our work is based on other recent studies. Firstly, the photo-induced temperature, which can be the source of thermal radiation, is calculated in multilayers for arbitrary spatio-temporal illumination [14]. This calculation is based on an optical/thermal analogy [15]. We then extended the direct methods in the case of multilayers [16] to calculate the thermal Poynting flux radiated

#516952 https://doi.org/10.1364/OE.516952
Journal © 2024 Received 4 Jan 2024; revised 16 Feb 2024; accepted 17 Feb 2024; published 18 Mar 2024

Optics EXPRESS

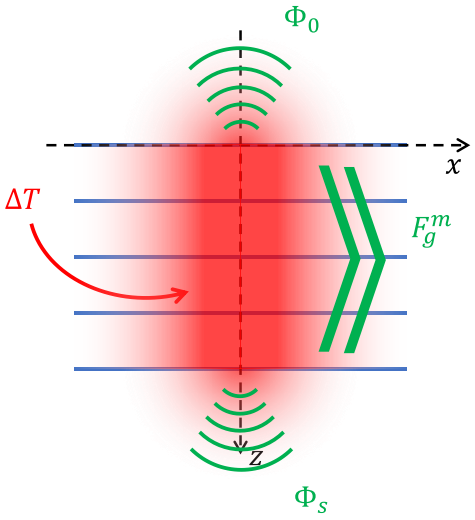

Fig. 1. Schematic diagram of the coupling of thermal radiation to the guided modes of the multilayer structure. In red is the heat source (temperature rise ΔT) resulting from the absorption of external illumination. This rise is responsible for thermal radiation propagating in the extreme media (superstrate Φ_0 and substrate Φ_s) but also in the form of guided modes (F_g^m).

by this temperature in free space, in the surrounding media which are the superstrate and the substrate. This flux calculation is carried out by introducing thermal currents (electrical and magnetic) into Maxwell's equations, based on the fluctuation-dissipation theorem [2–4,7–10]. However, we will see that this flux is not a suitable quantity for calculating the energy carried by the guided modes; for that reason we need to consider another quantity in this work, which is the electromagnetic power radiated by the thermal currents. The spectral density of this power is analyzed in the different frequency windows, and in particular in the modal window in which the guided modes are located (Fig. 2).

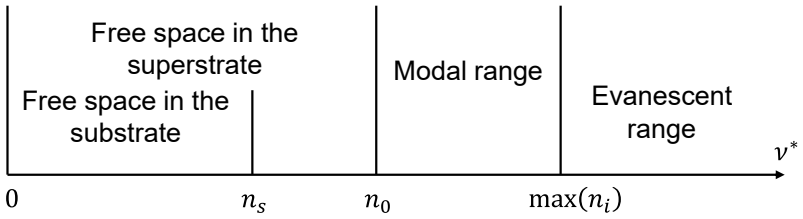

Fig. 2. Frequency windows for free space, guided modes and evanescent waves. The abscissa is the normalized spatial frequency [5], with n_0 and n_s the indices of the superstrate and substrate, and n_i the indices of the layers in the stack. Case $n_0 > n_s$.

This article is therefore devoted to the electromagnetic modelling of the trapped (or guided) thermal radiation in optical multilayers, whether photo-induced or not. In section 2 we briefly review the basic modelling [16] used to calculate the radiated field in free space, based on the tools conventionally used to design interference filters [5,6]. These bases are then extended in section 3 to obtain the expression of the double spectral density of electromagnetic power [5,17,18]. In section 4 this double density is shown to give access to the calculation of the

Optics EXPRESS

radiation trapped in each mode of the multilayer. Numerical results are given for a multi-dielectric mirror at thermal equilibrium, before concluding in section 5.

2. Free-space electromagnetic modelling of photo-induced thermal radiation in multilayers

In this section we briefly review the main results from the modelling [16] of the flux carried by thermal radiation in free space. This is necessary as we will need some expressions to move on to the power calculation in section 3. The component studied is a multilayer interference filter [5,6] made of materials assumed to be linear, homogeneous, isotropic and non-magnetic. These assumptions are typical of interference filters manufactured today using optical thin-film technologies [6,19,20]. Figure 3 shows the geometry of the multilayer system studied. The complex indices and thicknesses of the layers are given as n_i and e_i for each thin layer.

The approach can be summarized as follows. It is based on the electromagnetic modelling of thermal radiation introduced by Rytov in [2] and widely developed subsequently [7–11]. Molecular agitation is modelled by volume current densities which are related to temperature in accordance with the fluctuation-dissipation theorem [2–4]. The temperature can be the ambient temperature, or the photo-induced temperature following optical illumination of the component [14]. The thermal currents are then introduced into Maxwell's equations, which are solved to obtain the electromagnetic field characteristic of thermal radiation. This makes it possible to extract the value of the electromagnetic field for each temporal and spatial frequency, as well as the Poynting flux through a plane of altitude z in the far field. For simplicity, we will restrict ourselves to the S or TE polarization of the thermal radiation. This first step, which leads to the calculation of the thermal flux propagating in free space (outside the component, i.e. in the substrate and superstrate) through a z-altitude plane, is essential before tackling section 3, which deals with electromagnetic power and guided modes.

2.1. Thermal currents

The incident optical source is assumed to be quasi-monochromatic and collimated. It may be a pulsed source (single pulse or repeating), or a continuous source. When the multilayer component is illuminated by this source, part of the incident power is absorbed in the volume of the component and causes a photo-induced temperature rise $\Delta T(\vec{r}, z, t)$, where $\vec{r} = (x, y)$ designates the transverse variable and z the depth (see Fig. 3), with t the time variable. To calculate this temperature, we use the classical heat equation in the presence of a volume source given by the absorption volume density dA/dz in the multilayer [14]. The temperature field then defines a current density that is introduced into Maxwell's equations [2–4,7–11]. We restrict ourselves to non-magnetic materials as most often in optical interference coatings. Under these conditions, the current is electrical in nature and its analytical expression is obtained, on each axis and in each layer numbered (i), by the fluctuation-dissipation theorem [2,3]. We obtain, for an element of volume δV in each layer i:

$$\forall u \in \{x, y, z\}, \quad \tilde{J}_{u,i}(f, \vec{r}, z)\ \sqrt{\delta V}\ = e^{j\varphi^{J}_{u,i}(f,\vec{r},z)} \sqrt{4\pi f\ \Theta[2\pi f, T_i(\vec{r}, z)]\tilde{\epsilon}_i''(f)} \tag{1}$$

with:

$$\Theta(\omega = 2\pi f, T) = \frac{\bar{h}\omega}{e^{\frac{\bar{h}\omega}{k_B T}} - 1} \tag{2}$$

In these expressions (1) and (2), $\bar{h}$ and k_B are the reduced Planck and Boltzmann constants respectively, and $\tilde{\epsilon}_i''$ denotes the imaginary part of the Fourier Transform (FT) of the dielectric permittivity of the medium i. The electric current density $\tilde{J}_{u,i}$ is given in the first Fourier plane,

Optics EXPRESS

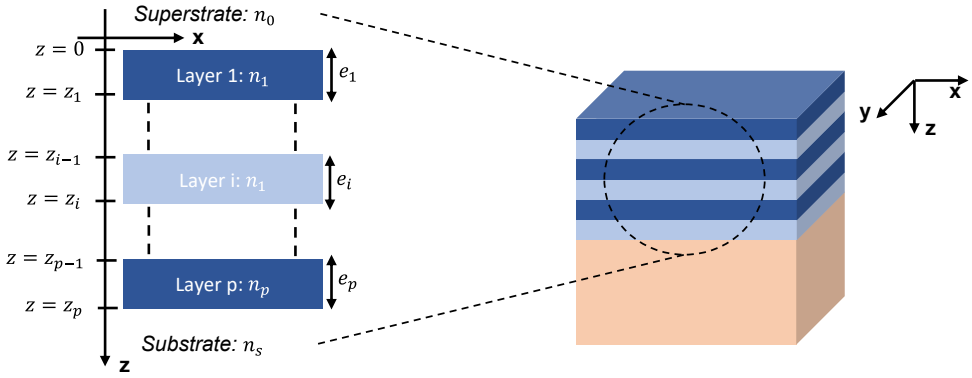

Fig. 3. General structure of a planar multilayer stack

i.e. after FT with respect to the time variable t. The time frequency is f, the Fourier variable conjugate to t. With a time dependence in $e^{-j2\pi ft}$, this FT is chosen as :

$$\tilde{X}(f) = \int_t X(t)e^{j2\pi ft}\,dt \Leftrightarrow X(t) = \int_f \tilde{X}(f)e^{-j2\pi ft}\,df \tag{3}$$

Note that the temperature in (1) and (2) writes as $T_i = T_a + \Delta T$, with T_a the ambient temperature. Finally, the quantity $\varphi^J_{u,i}$ in (1) represents the spectral phase of the electric current volume density $\tilde{J}_{u,i}$. This phase is a random variable that reflects the stochastic behaviour of the molecular agitation inside the component [3]. The statistical nature of its distribution makes it possible to take into account the independence of currents between two points in space or at different frequencies [3]. Another way of taking this independence into account is to consider Dirac distributions in the fluctuation-dissipation theorem [2,3].

It must be stressed that we here consider pulsed optical illumination with a pulse duration greater than one nanosecond, in order to guarantee local thermodynamic equilibrium [11]. Under these conditions, the spatio-temporal variations in temperature are much greater than the thermalization time (temporal aspect) and the mean free path (spatial aspect) of the diffusion process [4,21]. Thus, a temperature can be defined at each instant and at each location, and expression (1) remains valid in the space-time regime. This is why time is a dummy variable in equations (1,2). Indeed we are working on the assumption of linearity, so that the coating emissivity does not depend on the temperature. Furthermore, the coating properties are achromatic over the narrow bandwidth of the quasi-monochromatic incident beam. Consequently, the time response of the thermal radiation is simply proportional to that of the temperature [16]. In other words, for a transient response, it will suffice to multiply the results given in this work by the normalized time response of the temperature.

The current densities given by (1) and (2) are finally introduced into Maxwell's equations to calculate the radiated flux in free space. In the following section 2.2, we briefly review the calculation procedure developed in [16].

2.2. *Electromagnetic field radiated by the thermal currents*

This calculation requires to consider the second Fourier plane and therefore to introduce a second Fourier transform, namely the spatial FT (with respect to the variable $\vec{r}$) of the fields and sources. This step is necessary to take into account the transverse distribution (with limited support) of the incident beam, as well as to use the concepts of complex admittance and effective index [5], which are defined for a given temporal frequency and spatial frequency. The spatial FT is chosen

Optics EXPRESS

as:

$$\hat{X}(f,\vec{v},z)=\int_{\vec{r}}\tilde{X}(f,\vec{r},z)e^{-j2\pi\vec{v}.\vec{r}}d\vec{r}\Leftrightarrow\tilde{X}(f,\vec{r},z)=\int_{\vec{v}}\hat{X}(f,\vec{v},z)e^{j2\pi\vec{v}.\vec{r}}d\vec{v} \tag{4}$$

where $\vec{v}$ is the spatial frequency, i.e. the conjugate Fourier variable of the space transverse variable $\vec{r}$.

The calculation of the S-polarized electromagnetic field created by an arbitrary volume density of electric current in a multilayer is detailed in [22]. Here we recall the expression for the field created by the volume of layer i of thickness e_i limited by interfaces z_{i-1} and z_i. This field is expressed at the upper ($z=z_i$) and at the lower ($z=z_{i-1}$) interfaces, that is:

$$\begin{array}{rcl}\overrightarrow{\hat{E}}_{i,i-1} & = & \frac{1}{\Delta Y_{i-1}}[G^0_{1i}\overrightarrow{\hat{E}}^g_i(z_i)+G^0_{2i}\overrightarrow{\hat{E}}^g_i(z_{i-1})]\\ \overrightarrow{\hat{E}}_{i,i} & = & \frac{1}{\Delta Y_i}[G^s_{1i}\overrightarrow{\hat{E}}^g_i(z_i)+G^s_{2i}\overrightarrow{\hat{E}}^g_i(z_{i-1})]\end{array} \tag{5}$$

with $\Delta Y_i=Y_i-Y'_i$, $G^0_{1i}=(\tilde{n}_i-Y_{i-1})e^{-j\delta_i}$, $G^0_{2i}=\tilde{n}_i+Y_{i-1}$, $G^s_{1i}=\tilde{n}_i-Y'_i$ et $G^s_{1i}=(\tilde{n}_i+Y'_i)e^{-j\delta_i}$, $\delta_i=\alpha_i e_i$, $\alpha_i=\sqrt{k_i^2-(2\pi\vec{v})^2}$, $k_i=\frac{2\pi n_i}{\lambda}$, where λ is the wavelength of thermal radiation.

In these expressions the admittances and effective indices are denoted by Y_i and $\tilde{n}_i$ respectively. Y_i denotes the admittance at interface i calculated by recurrence from the effective index $\tilde{n}_s$ of the substrate, while Y'_i denotes the admittance at interface i calculated by recurrence from the effective index $-\tilde{n}_0$ of the superstrate [5]:

$$\begin{cases}Y_p & = & \tilde{n}_s\\ \forall i\in\{1,\dots,p\}, Y_{i-1} & = & \frac{Y_i\cos\delta_i-j\tilde{n}_i\sin\delta_i}{\cos\delta_i-j\frac{Y_i}{\tilde{n}_i}\sin\delta_i}\quad .a)\end{cases} \tag{6.a}$$

$$\begin{cases}Y'_0 & = & -\tilde{n}_0\\ \forall i\in\{1,\dots,p\}, Y'_i & = & \frac{Y'_{i-1}\cos\delta_i+j\tilde{n}_i\sin\delta_i}{\cos\delta_i+j\frac{Y'_{i-1}}{\tilde{n}_i}\sin\delta_i}\quad .b)\end{cases} \tag{6.b}$$

Furthermore, in expression (5), the electric field $\overrightarrow{\hat{E}}^g_i$ is a particular solution of the Helmholtz equation in the second Fourier plane, in the case of a volume electric current density $\overrightarrow{\tilde{J}}_i$ in layer i. To recall, Helmholtz equation comes from Maxwell equations in the first Fourier plane (after a FT with respect to the time variable):

$$\begin{cases}\overrightarrow{\mathrm{rot}}(\overrightarrow{\tilde{E}}_i)=j\omega\mu_i\overrightarrow{\tilde{H}}_i\\ \overrightarrow{\mathrm{rot}}(\overrightarrow{\tilde{H}}_i)=-j\omega\epsilon_i\overrightarrow{\tilde{E}}_i+\overrightarrow{\tilde{J}}_i\end{cases}\Rightarrow\Delta\overrightarrow{\tilde{E}}_i+k_i^2\overrightarrow{\tilde{E}}_i=\overrightarrow{\tilde{S}}^{E_i} \tag{7}$$

where the source term is written as:

$$\overrightarrow{\tilde{S}}^{E_i}=-j\omega\mu_i\overrightarrow{\tilde{J}}_i+\frac{1}{j\omega\epsilon_i}\overrightarrow{\mathrm{grad}}[\mathrm{div}\ \overrightarrow{\tilde{J}}_i] \tag{8}$$

This solution $\overrightarrow{\hat{E}}^g_i$ of Eq. (7) is the result of the convolution product on the space variable z between the source term and the Green's function G_i associated with the Helmholtz equation. It

Optics EXPRESS

is written in the second Fourier plane as:

$$\overrightarrow{\hat{E}}_i^g = G_i *_z \overrightarrow{\hat{S}}^{E_i} \text{ with } G_i = \frac{1}{2j\alpha_i} e^{j\alpha_i |z|} \tag{9}$$

Then the spatial FT of this term in the basis $(\vec{x}, \vec{y})$ gives, in the second Fourier plane:

$$\overrightarrow{\hat{S}}^{E_i} = -j\omega\mu_i \begin{pmatrix} \left(1 - \frac{\sigma_x^2}{k_i^2}\right)\hat{J}_{x,i} - \frac{\sigma_x\sigma_y}{k_i^2}\hat{J}_{y,i} + j\frac{\sigma_x}{k_i^2}\frac{\partial \hat{J}_{z,i}}{\partial_z} \\ -\frac{\sigma_x\sigma_y}{k_i^2}\hat{J}_{x,i} + \left(1 - \frac{\sigma_y^2}{k_i^2}\right)\hat{J}_{y,i} + j\frac{\sigma_y}{k_i^2}\frac{\partial \hat{J}_{z,i}}{\partial_z} \end{pmatrix} \tag{10}$$

with $\vec{\sigma} = 2\pi\vec{\nu}$ the spatial pulsation. In the following we will note :

$$\overrightarrow{\hat{S}}^{E_i} = -j\omega\mu_i \begin{pmatrix} a_{xx}\hat{J}_{x,i} + a_{xy}\hat{J}_{y,i} + a_{xz}\frac{\partial \hat{J}_{z,i}}{\partial_z} \\ a_{yx}\hat{J}_{x,i} + a_{yy}\hat{J}_{y,i} + a_{yz}\frac{\partial \hat{J}_{z,i}}{\partial_z} \end{pmatrix} \tag{11}$$

Remember that, because of the S polarization to which we are limiting ourselves here, the electric field is tangential at the interfaces of the layers, so that it is continuous in the presence of volume sources. Note also that in the case of thermal radiation, it is the currents given by (1) that are involved in (11). Finally, the expression for the electric source term in (11), combined with (9), yields the particular solutions $\overrightarrow{\hat{E}}_i^g$ of the electric field involved in expression (5), giving access to the electric field produced by layer i on the upper ($\overrightarrow{\hat{E}}_{ii}$) and lower ($\overrightarrow{\hat{E}}_{ii-1}$) interfaces of layer i. From this field, it is then easy to calculate the flux of the Poynting vector in the emerging media (substrate and superstrate), using traversal coefficients [5] which depend on the admittances and effective indices.

To conclude this section, it should be noted that we do not use dyadic Green's functions [23] but work with Green's functions in the second Fourier plane. The two approaches give identical results with a similar level of complexity. Our choice to work in the second Fourier plane is due to the fact that it allows us to benefit from all the tools already developed for the synthesis [5] of thin film stacks, in particular complex admittances and effective indices.

2.3. Results from the stochastic properties of currents

Before calculating the power supplied by thermal currents, it is necessary to explain how their stochastic properties make it possible to simplify calculations of energy quantities (power, flux, absorption). These quantities are expressed using products between fields, or between fields and currents [5]. As the fields are expressed as a linear combination of spatial convolution products between the currents and Green's function (see expressions (5,9,11)), calculations of energy quantities give rise to expressions of the type:

$$\int_{z'}\int_{z''} L_i(\nu,\ z', z'')\hat{J}^*_{a,i}(\vec{\nu}, z')\hat{J}_{b,i}(\vec{\nu}, z'')dz'dz'' \ with\ \ a, b \in \{x, y, z\} \tag{12}$$

In this expression, $\hat{J}_{a,i}$ represents the a-axis component of the double spatial TF of the thermal current in layer (i) expressed in (1), and $\hat{J}^*_{a,i}$ is its complex congugate. L_i is a function depending on the integration variables z' and z'' as well as the modulus ν of the spatial frequency ($\nu = |\vec{\nu}|$).

The phase terms of the currents are assumed to be independent and uniformly distributed. This means that the thermal agitation at one point and along one axis is decorrelated from that at another point or along another axis. This property makes it possible to recover Dirac distributions in the expression of thermal currents [1–4]. In our case, it imposes quantity (12) to be zero for $a \neq b$. Moreover, in the case $a = b$, expression (12) reveals a difference between the phases of

Optics EXPRESS

the currents taken at two different altitudes z' and z''. As a result, expression (12) only integrates on the path defined by $z' = z''$ where the phases of the currents are identical, giving :

$$\int_{z'}\int_{z''} L_i(\nu,\ z', z'')\hat{J}^*_{a,i}(\vec{\nu}, z')\hat{J}_{a,i}(\vec{\nu}, z'')dz'dz'' = \int_{z'} L_i(\nu,\ z')|\hat{J}_{a,i}(\vec{\nu}, z')|^2 dz' \tag{13}$$

To go further, we need to use the expressions for thermal currents which are given in the first Fourier plane (see Eq. (1)). To do this, we use the inverse TF of the current $\hat{J}_{a,i}$, which gives a double integral over the transverse spatial variables $\vec{r}$ and $\vec{r}'$ in expression (13). We then use the same reasoning as before to reduce this integration on the path $\vec{r} = \vec{r}'$. This gives us:

$$\int_{z'} L_i(\nu,\ z')|\hat{J}_{a,i}(\vec{\nu}, z')|^2 dz' = \int_{z'} L_i(\nu,\ z') \int_{\vec{r}} |\tilde{J}_{a,i}(\vec{r}, z')|^2 d\vec{r}dz' \tag{14}$$

Finally, using expression (1) of the currents we get the following result :

$$\begin{array}{l} \forall a, b \in \{x, y, z\}, \\ \int_{z'}\int_{z''} L_i(\nu,\ z', z'')\hat{J}^*_{a,i}(\vec{\nu}, z)\hat{J}_{b,i}(\vec{\nu}, z')dz'dz'' \ = \\ \begin{cases} 0 & \text{if } \ a \neq b \\ 4\pi f \tilde{\varepsilon}_i''(f) \int_z L_i(\nu,\ z)dz \int_{\vec{r}} \Theta(2\pi f, T_i(\vec{r}, z_i))d\vec{r} & \text{else} \end{cases} \end{array} \tag{15}$$

3. Calculation of the power supplied by thermal currents and application to guided modes

Once the expressions for the sources and fields are known for thermal radiation, the power F supplied by these sources in the far field can be calculated in a similar way to that used for optical micro-cavities [5,17,18] or trapped light scattering [24]. If absorption A could be neglected, this power could be written as $F = \Phi + \Phi_g$, with Φ the flux radiated in free space in the surrounding media and Φ_g the guided flux transported by the modes parallel to the interfaces of the structure. However, the presence of thermal radiation implies the presence of absorption, so the power balance in the far field must be written as $F = \Phi + A$, since the modes are absorbed during their propagation. Strictly speaking, this balance could be broken down into three components of absorption, i.e. $A = A_{low} + A_g + A_{ev}$, where A_{low} designates the absorption corresponding to the low spatial frequencies of the field characteristic of free space, A_g the absorption due to the attenuation of guided modes in the modal window (Fig. 2), and A_{ev} the dissipative part linked to evanescent waves in an absorbing medium. It should be remembered that while evanescent waves do not transport energy in a transparent medium, they do contribute to the absorption budget in a dissipative medium [5].

In the end, this means that it will be necessary to work with the double spectral density of power in order to distinguish the different frequency windows [5,17,18,24]. The aim of this section 3 is to demonstrate the analytical expression of this density. This double power density will then be used in section 4 to calculate to the coupling efficiency, analytically and numerically.

It should also be emphasized that our previous work [16] on the thermal radiation emerging from the component towards the superstrate and substrate was based on the calculation of the far field flux of the Poynting vector in free space, through a plane of normal $\pm\vec{z}$ and at altitude $\pm z$. This type of calculation is no longer appropriate here, as the modes transport energy through azimuthal (or polar) planes whose normals lie is in the xy plane. Under these conditions, a similar Poynting flux calculation would be tricky because of the discontinuity in the physical properties of the different media. Conversely, calculating the power density supplied by the sources makes it possible to simplify and solve this problem (as in the case of trapped scattering [24]), while taking account of the coupling efficiency in the modes.

Optics EXPRESS

3.1. Power density supplied by a bulk distribution of electric current

We take as our starting point results from the field of optical micro-cavities [5,17,18,25], which give the expression for the power F supplied by a bulk electrical current distribution in a multilayer component. In terms of spectral density, or per unit of temporal and spatial frequency, this can be written for all-dielectric multilayers as [5]:

$$\frac{\partial F}{\partial f \partial \vec{\nu}} = -2 \sum_{i=1}^{p} \int_{z=z_{i-1}}^{z_i} \Re\{\overrightarrow{\hat{J}}_i^*(f, \vec{\nu}, z).\overrightarrow{\hat{E}}_i(f, \vec{\nu}, z)\} dz \tag{16}$$

where $\overrightarrow{\hat{J}}_i$ is the electric volume current of layer i, $\overrightarrow{\hat{J}}_i^*$ its conjugate and $\overrightarrow{\hat{E}}_i$ the field radiated by this current. To obtain (16), it has been assumed that the currents in the different layers ($j \neq i$) do not interfere (see Section 2.3), which is consistent with the thermal radiation framework [1]. We also note in (16) that the quantities are given in the second Fourier plane (after a double FT).

3.2. Taking polarization into account

To develop the calculations further, it is necessary to analyze the polarization of the emitted radiation, which is defined in the second Fourier plane where the wave vectors are defined. The field is thus decomposed in the $(\vec{\nu}, z)$ plane using the diagram in Fig. 4, where the unit vectors $\vec{u}$ and $\vec{w}$ are defined as :

$$\vec{u} = \frac{\vec{\nu}}{\nu} = (\cos\phi, \sin\phi) \qquad \vec{w} = \left(\frac{1}{\nu}\right)\left(\frac{\partial \vec{\nu}}{\partial \phi}\right) = (-\sin\phi, \cos\phi) \tag{17}$$

For S polarization, the electric field is perpendicular to $\vec{u}$. Hence we can write:

$$\overrightarrow{\hat{E}}_i^S = (-\hat{E}_{x,i}\sin\phi + \hat{E}_{y,i}\cos\phi)\vec{w} \tag{18}$$

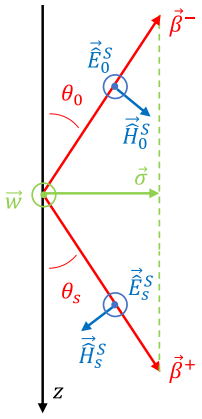

Fig. 4. Schematic representation, for S polarization, of the normal angle θ defining the wave vector $\beta^{\pm}$ of the retrograde electric field $\overrightarrow{\hat{E}}_0$ in the superstrate, and the progressive field $\overrightarrow{\hat{E}}_s$ in the substrate. The spatial pulsation $\vec{\sigma} = 2\pi\vec{\nu}$ is the tangential component common to the 2 wave vectors.

Optics EXPRESS

And so, in the $(\vec{x}, \vec{y})$ basis:

$$\overrightarrow{\hat{E}}_i^S = \begin{pmatrix} \hat{E}_{x,i}\sin^2\phi - \hat{E}_{y,i}\cos\phi\sin\phi \\ -\hat{E}_{x,i}\sin\phi\cos\phi + \hat{E}_{y,i}\cos^2\phi \end{pmatrix} \tag{19}$$

Therefore, following (19) et (16), the double spectral density of power follows for S polarization:

$$\begin{aligned} \frac{\partial F}{\partial f \partial \vec{\nu}} = -2R \Big\{ \sum_{i=1}^{p} \int_z \hat{J}_{x,i}^* (\hat{E}_{x,i}\sin^2\phi - \hat{E}_{y,i}\sin\phi\cos\phi) \\ + \hat{J}_{y,i}^* (-\hat{E}_{x,i}\sin\phi\cos\phi + \hat{E}_{y,i}\cos^2\phi)\, dz \Big\} \end{aligned} \tag{20}$$

3.3. Homogeneous and particular contributions

In order to continue the development, the electric field must be decomposed into its particular and homogeneous solutions, which are written as:

$$\overrightarrow{\hat{E}}_i = \overrightarrow{\hat{E}}_i^h + \overrightarrow{\hat{E}}_i^g \tag{21}$$

We have already seen that the particular solution $\overrightarrow{\hat{E}}_i^g$ is expressed using Eq. (9). As for the homogeneous solution $\overrightarrow{\hat{E}}_i^h$, it is expressed in each layer i as [5] :

$$\overrightarrow{\hat{E}}_i^h(z) = \frac{1}{\sin\delta_i}[\overrightarrow{\hat{E}}_i^h(z_i)\sin(\alpha_i(z - z_{i-1})) + \overrightarrow{\hat{E}}_i^h(z_{i-1})\sin(\alpha_i(z_i - z))] \tag{22}$$

with the phase term $\delta_i = \alpha_i e_i$. Given (21), we can introduce the fields $\overrightarrow{\hat{E}}_{i,i}$ and $\overrightarrow{\hat{E}}_{i,i-1}$ on the upper and lower interfaces of layer i, whose expressions are known from (5). We obtain the analytical expression of the homogeneous solution as:

$$\begin{aligned} \overrightarrow{\hat{E}}_i^h(z) = \frac{1}{\sin\delta_i}[(\overrightarrow{\hat{E}}_{ii} - \overrightarrow{\hat{E}}_i^g(z_i))\sin(\alpha_i(z - z_{i-1})) \\ +(\overrightarrow{\hat{E}}_{ii-1} - \overrightarrow{\hat{E}}_i^g(z_{i-1}))\sin(\alpha_i(z_i - z))] \end{aligned} \tag{23}$$

At this stage the homogeneous $\overrightarrow{\hat{E}}_i^h(z)$ and particular $\overrightarrow{\hat{E}}_i^g(z)$ fields are known at any altitude. This makes it possible to decompose the power density given in (16) into a homogeneous contribution and a particular contribution corresponding respectively to these components, that is:

$$\begin{aligned} \frac{\partial F}{\partial f \partial \vec{\nu}} &= \frac{\partial F^h}{\partial f \partial \vec{\nu}} + \frac{\partial F^g}{\partial f \partial \vec{\nu}} \\ &= -2\sum_{i=1}^{p} \int_{z=z_{i-1}}^{z_i} \Re\{\overrightarrow{\hat{J}}_i^*(f, \vec{\nu}, z).\overrightarrow{\hat{E}}_i^h(f, \vec{\nu}, z)\} dz \\ &\quad - 2\sum_{i=1}^{p} \int_{z=z_{i-1}}^{z_i} \Re\{\overrightarrow{\hat{J}}_i^*(f, \vec{\nu}, z).\overrightarrow{\hat{E}}_i^g(f, \vec{\nu}, z)\} dz \end{aligned} \tag{24}$$

Optics EXPRESS

3.3.1. Calculation of the particular contribution

Relations (20) gives, for the particular power contribution :

$$\begin{aligned}\frac{\partial F^g}{\partial f\partial\vec{\nu}} = -2\sum_{i=1}^{p}\int_{z=z_{i-1}}^{z_i} \Re\{\hat{J}^*_{x,i}(z)(\hat{E}^g_{x,i}(z)\sin^2\phi - \hat{E}^g_{y,i}(z)\sin\phi\cos\phi)\\ + \hat{J}^*_{y,i}(z)(-\hat{E}^g_{x,i}(z)\sin\phi\cos\phi + \hat{E}^g_{y,i}(z)\cos^2\phi)\}dz\end{aligned} \tag{25}$$

Recall that the particular solution of the field can be written, in accordance with Eqs. (6) and (11), as:

$$\begin{aligned}&\forall a \in \{x,y\},\ \forall z \in [z_{i-1}, z_i],\\ &\hat{E}^g_{a,i}(z) = -j\omega\mu_i \int_{z'=z_{i-1}}^{z_i} G_i(z-z')\left(a_{ax}\hat{J}_{x,i}(z') + a_{ay}\hat{J}_{y,i}(z') + a_{az}\frac{\partial \hat{J}_{z,i}}{\partial_z}(z')\right)dz'\end{aligned} \tag{26}$$

Taking into account the properties introduced in section 2.3, and the expression for the currents given in (1,2), we then find:

$$\begin{aligned}\frac{\partial F^g}{\partial f\partial\vec{\nu}} = 2\sum_{i=1}^{p}\Re\Big\{&j\omega\mu_i 4\pi f\tilde{\varepsilon}''_i \int_{\vec{r}}\Theta(2\pi f, T_i(\vec{r}, z_i))d\vec{r}\\ &[a_{xx}\sin^2\phi - (a_{yx}+a_{xy})\sin\phi\cos\phi + a_{yy}\cos^2\phi]\int_{z=z_{i-1}}^{z_i} G_i(0)dz\Big\}\end{aligned} \tag{27}$$

Furthermore we have :

$$a_{xx}\sin^2\phi - (a_{yx}+a_{xy})\sin\phi\cos\phi + a_{yy}\cos^2\phi = 1 \quad and \quad \int_{z=z_{i-1}}^{z_i} G_i(0)dz = \frac{e_i}{2j\alpha_i} \tag{28}$$

So that, introducing the effective index $\tilde{n}_i = \alpha_i/\omega\mu_i$ of layer i for S polarization [5], we get:

$$\frac{\partial F^g}{\partial f\partial\vec{\nu}} = 2\sum_{i=1}^{p}\Re\left\{\frac{1}{\tilde{n}_i}\right\}\frac{e_i}{2}4\pi f\tilde{\varepsilon}''_i\int_{\vec{r}}\Theta(2\pi f, T_i(\vec{r}, z_i))d\vec{r} \tag{29}$$

It should be noted that this formula of the particular power component does not directly involve the optical admittances of the stack, but the effective indices, imaginary permittivities and thicknesses. This would mean that the overall optical interference balance of the multilayer does not come into play for that contribution, since any arrangement of the layers would give the same result. However this is no true because the admittances still intervene via the temperature which can follow the stationary optical field in the case of short pulses [14]. We will see that the situation is different for the homogeneous component in the next sub-section.

3.3.2. Calculation of the homogeneous contribution

In the same way, for the homogeneous solution, we have from (20):

$$\begin{aligned}\frac{\partial F^h}{\partial f\partial\vec{\nu}} = -2\sum_{i=1}^{p}\int_{z=z_{i-1}}^{z_i} \Re\{\hat{J}^*_{x,i}(z)(\hat{E}^h_{x,i}(z)\sin^2\phi - \hat{E}^h_{y,i}(z)\sin\phi\cos\phi)\\ + \hat{J}^*_{y,i}(z)(-\hat{E}^h_{x,i}(z)\sin\phi\cos\phi + \hat{E}^h_{y,i}(z)\cos^2\phi)\}dz\end{aligned} \tag{30}$$

The expression for the homogeneous solution of the electric field is given by (5) and (23) and can be expanded as follows:

$$\begin{aligned}\overrightarrow{\hat{E}}^h_i(z) = &\tfrac{\sin(\alpha_i z)}{\Delta Y_i\sin\delta_i}((G^s_{1i} - \Delta Y_i)\overrightarrow{\hat{E}}^g_i(e_i) + G^s_{2i}\overrightarrow{\hat{E}}^g_i(0))\\ &+\tfrac{\sin(\alpha_i(e_i-z))}{\Delta Y_{i-1}\sin\delta_i}(G^0_{1i}\overrightarrow{\hat{E}}^g_i(e_i) + (G^0_{2i} - \Delta Y_{i-1})\overrightarrow{\hat{E}}^g_i(0))\end{aligned} \tag{31}$$

Optics EXPRESS

Then, noting that we can write,

$$\begin{aligned}
&\forall a \in \{x, y\},\\
&\hat{E}^g_{a,i}(0) = -j\omega\mu_i \int_{z'=z_{i-1}}^{z_i} G_i(z_{i-1} - z') \left(a_{ax}\hat{J}_{x,i}(z') + a_{ay}\hat{J}_{y,i}(z') + a_{az}\frac{\partial \hat{J}_{z,i}}{\partial_z}(z') \right) dz'\\
&\overrightarrow{\hat{E}^g_i}(e_i) = -j\omega\mu_i \int_{z'=z_{i-1}}^{z_i} G_i(z_i - z') \left(a_{ax}\hat{J}_{x,i}(z') + a_{ay}\hat{J}_{y,i}(z') + a_{az}\frac{\partial \hat{J}_{z,i}}{\partial_z}(z') \right) dz'
\end{aligned} \tag{32}$$

and again using the properties described in section 2.3:

$$\frac{\partial F^h}{\partial f \partial \vec{\nu}} = 2 \sum_{i=1}^{p} 4\pi f \tilde{\epsilon}_i'' \int_{\vec{r}} \Theta(2\pi f, T_i(\vec{r}, z_i)) d\vec{r} \tag{33}$$

$$\Re \left\{ \frac{1}{2\tilde{n}_i \sin\delta_i} \left[\frac{1}{\Delta Y_i}(I_{2i}(G^s_{1i} - \Delta Y_i) + I_{1i}G^s_{2i}) + \frac{1}{\Delta Y_{i-1}}(I_{4i}G^0_{1i} + I_{3i}(G^0_{2i} - \Delta Y_{i-1})) \right] \right\}$$

with :

$$\begin{cases}
I_{1i} = \int_{z=z_{i-1}}^{Z_i} \sin(\alpha_i(z - z_{i-1}))\, e^{j\alpha_i|z_{i-1}-z|} dz = \frac{1+2j\delta_i - e^{2j\delta_i}}{4\alpha_i}\\
I_{2i} = \int_{z=z_{i-1}}^{Z_i} \sin(\alpha_i(z - z_{i-1}))\, e^{j\alpha_i|z_i-z|} dz = \frac{(1-2j\delta_i - e^{-2j\delta_i})e^{j\delta_i}}{4\alpha_i}\\
I_{3i} = \int_{z=z_{i-1}}^{z_i} \sin(\alpha_i(z_i - z))\, e^{j\alpha_i|z_{i-1}-z|} dz = I_{2i}\\
I_{4i} = \int_{z=z_{i-1}}^{z_i} \sin(\alpha_i(z_i - z))\, e^{j\alpha_i|z_i-z|} dz = I_{1i}
\end{cases} \tag{34}$$

This time, in contrast to the particular component of the power given in (29), the expression (33) of the homogeneous component of the power involves terms closely related to the multilayer formula, in particular through the admittances and their differences. This homogeneous power can be strongly achromatic or dispersive.

3.4. Final expression for the power spectral density

Finally, using the quantities G from Eq. (5), and summing the homogeneous and particular contributions, we obtain the following expression for the surface power density supplied per unit frequency f and spatial frequency $\vec{\nu}$:

$$\begin{aligned}
\frac{\partial F}{\partial f \partial \vec{\nu} \partial S} = 2 \sum_{i=1}^{p} 4\pi f \tilde{\epsilon}_i'' \Re \left\{ \frac{1}{2\tilde{n}_i \sin\delta_i} \left[\frac{1}{\Delta Y_i}(I_{2i}(\tilde{n}_i - Y_i) + I_{1i}(\tilde{n}_i + Y_i')e^{-j\delta_i}) \right.\right.\\
= \left.\left. + \frac{1}{\Delta Y_{i-1}}(I_{1i}(\tilde{n}_i - Y_{i-1})e^{-j\delta_i} + I_{2i}(\tilde{n}_i + Y_{i-1}')) + e_i \sin\delta_i \right] \right\} \Theta(2\pi f, T_i(\vec{r}, z_i))
\end{aligned} \tag{35}$$

A classical change of variable then gives the power density supplied per unit modulus of spatial frequency $\nu = |\vec{\nu}|$ and polar angle ϕ[5], i.e. :

$$\frac{\partial F}{\partial f \partial \nu \partial \phi \partial S} = \nu \frac{\partial F}{\partial f \partial \vec{\nu} \partial S} \tag{36}$$

It is this quantity (analogous to the radiative spectral intensity [1]) that will be calculated and plotted in the next section. Note that it is isotropic, i.e. independent of the angle ϕ.

4. Numerical calculation

4.1. Method

The double power density expressed in (35-36) will be plotted as a function of the normalized frequency $\nu^* = \lambda\nu$, which is homogeneous to a refractive index. Note that for a real index medium satisfying $n_i < \nu^*$, this quantity can be written as $\nu^* = n_i sin\theta_i$. Different frequency windows can then be distinguished [5] (see Fig. 2):

Optics EXPRESS

- Low frequencies characteristic of plane waves emerging in free space in the superstrate ($0<\nu^*<n_0 = 1$) and in the substrate ($0<\nu^*<n_s = 1.52$)
- The modal window ($\max(n_0, n_s)<\nu^*<\max(n_i)$) where the characteristic constants of the guided modes are found when they exist, and where $\max(n_i)$ is taken over all the indices of the thin layers of the multilayer
- Evanescent waves ($\max(n_i)<\nu^*$) which do not transport energy in the supposedly transparent emergence media, but contribute to the loss balance in the dissipative multilayer.

As a reminder, in the absence of absorption the flux and power densities would be identical in free space in the emergent media for low frequencies, which we have verified (analytically and numerically) with decreasing imaginary indices. It is therefore essentially the modal window that interests us here, where the power density (conversely to the flux) can be calculated so as to highlight the coupling efficiency to the guided modes. When existing, the modal constants ν_m^* can be found in this window. These constants are the poles of the reflection factor $r(\nu)$ of the stack [5,24] and can therefore be obtained simply from equation $\frac{1}{r(\nu)} = 0$.

Thus, at a temporal frequency $f = c/\lambda$, the total power P_g transferred to the guided modes is given by the integral of the power density in the modal window, i.e. :

$$P_g(\lambda) = \frac{\partial F}{\partial f \partial S} = \int_\phi \int_\nu \frac{\partial F}{\partial f \partial \nu \partial \phi \partial S} d\nu d\phi = 2\pi \int_{\max(n_0,n_s)}^{\max(n_i)} \nu^* \frac{\partial F}{\partial f \partial \vec{\nu}^* \partial S} d\nu^* \tag{37}$$

Note that the density $\nu^* \frac{\partial F}{\partial f \partial \vec{\nu}^*}$ does not present any singularity. Indeed, this quantity has the same poles ν_m^* as those of the reflection factor, due to the presence of terms in $\frac{1}{\Delta Y_i}$ and $\frac{1}{\Delta Y_{i-1}}$ in (35). Indeed, it is known that [25]:

$$\frac{1}{r(\nu)} = 0 \leftrightarrow \forall i, z \;\; \Delta Y_i(\nu, z) = 0 \tag{38}$$

As a reminder, the modes in layer (i) of the multilayer are expressed in the second Fourier plane as $\vec{E}_{im}(\vec{r}, z) = \vec{A}_{im}(z) e^{j2\pi \vec{\nu}_m . \vec{r}}$, where ν_m is solution of (38) and $\vec{\nu}_m = \nu_m(\cos\phi, \sin\phi)$. If the media were perfectly transparent, the poles ν_m^* would be real and would create singularities; in this case, we would have to use the residue theorem to calculate the integral P_g at each wavelength. However, in the case of thermal radiation, materials are necessarily dissipative since their absorption is at the source of the radiation. Consequently, the poles of the power density have a non-zero imaginary part and prevent it from diverging. Note also that for the same reason the sinus term in (35) cannot be zero. There is therefore no singularity in the power density, and we can proceed in a different way to the residue theorem. All we have to do is numerically integrate the power density in the vicinity of the real part of the poles, where the maxima are located. This gives the energy transferred to the guided modes. Note that given the low absorptions of specific infrared materials (G_e, B_aF_2) that we will consider, these poles are located close to the real axis. Finally, we obtain:

$$P_g(\lambda) = \sum_{m=1}^{m=q} P_g^m(\lambda) \;\; = 2\pi \sum_{m=1}^{m=q} \int_{\nu_m^* - \frac{\Delta\nu_m^*}{2}}^{\nu_m^* + \frac{\Delta\nu_m^*}{2}} \nu^* \frac{\partial F}{\partial f \partial \vec{\nu}^* \partial S} d\nu^* \tag{39}$$

where q is the number of modes at wavelength λ, ν_m^* the modal constant of the m-th mode at this wavelength, and $\Delta\nu_m$ the width of the resonance around the pole ν_m^*. For the calculation of integrals around the modal frequencies, the bandwidth $\Delta\nu_m^*$ is chosen as the difference between the two frequencies on either side of the frequency where the density is maximum, each of these frequencies giving rise to an attenuation of a factor of 100.

Optics EXPRESS

For the numerical calculations that follow, for the sake of simplicity and presentation, we will consider the simple case of a uniform temperature in the component (T = 20°C). The model developed so far obviously remains valid in this particular case of thermal equilibrium. It should be noted that the uniform temperature can be ambient or photo-induced using a pulsed source with a duration greater than 1 ms.

4.2. Case of a quarter-wave multi-dielectric mirror

Consider a multi-dielectric mirror (sometimes described by some within the community as a 1D photonic crystal) designed at normal illumination for the mid-infrared range, comprising 5 quarter wave layers at the design wavelength $\lambda_0 = 2\mu m$, of formula $H(LH)^2$ and deposited onto a Z_nS_e substrate. In the mirror formula, H represents a layer of a high index material (G_e), while L is used for a low index material (B_aF_2). The real optical thicknesses of the H and L layers follow $n_H e_H = n_L e_L = \frac{\lambda_0}{4}$. Due to the high index ratio (n_H/n_L) in the MIR range, a small number of layers is sufficient to achieve high reflection ($R \approx 99$ %) at the design wavelength λ_0. The optical parameters of the media are summarized in Table 1 [26]. Note that G_e, B_aF_2 and Z_nS_e have slight index dispersion in the MIR range, for which reason we use their average index values. These index values (and notably the imaginary index - here taken at 10^{-4} for the thin films) may depend on the deposition conditions and technology. Absorption in the Z_nS_e substrate is not considered.

Table 1. Optical parameters used for numerical calculation

Materials	B_aF_2	G_e	*Air*	Substrate: Z_nS_e
Average MIR refractive index	$1.45 + j10^{-4}$	$4.0 + j10^{-4}$	1.0	2.4

The results are given in Fig. 5 at a wavelength λ equal to the design (or central) wavelength λ_0 of the filter, that is, $\lambda = \lambda_0 = 2\mu m$. We first note the low values of the power spectral density (blue curve), due to the low value of the imaginary indices (10^{-4}) and to the moderate value of the ambient temperature (20°C). In the free space window ($0<\nu^*<2.4$), we plotted the flux densities for free space in reflection (solid red curve, $0<\nu^*<1$) and in transmission (dashed green curve, $0<\nu^*<2.4$). The sum of these 2 flux densities is slightly less than the power density (solid blue curve), the small difference being due to the low absorption obtained with $n''_H = n''_L = 10^{-4}$. This is noted to check the consistency of the results. Furthermore, in the modal window ($2.4<\nu^*<4$) shown by the black vertical bars, we can clearly see the maxima characteristic of the presence of 3 poles in the vicinity of the real axis. These maxima obviously increase as the imaginary index decreases, at the same time as the width of the peaks. Finally, at the highest frequencies ($4<\nu^*$), we find the weight of the dissipation caused by evanescent waves, of the order of 5. 10^{-4} of the energy radiated in free space.

As announced in Section 4.1, it is sufficient to integrate the power density in the vicinity of each of the poles to obtain the energy transferred to each mode before attenuation. The results are given in Table 2. In this table the values of the integrals $P_g^m(\lambda = \lambda_0)$ for each mode of order m are normalized to the integral of the power in free-space, which makes it possible to highlight the relative weight of the trapped powers compared with the emerging free-space fluxes. It can be seen here that the modal power is globally equi-distributed between the 3 modes $TE_{i=1,2,3}$, and that each mode is transferred a power greater than that of free space, by a factor greater than 3.

The normalized sum of the power trapped by all the modes is 12.32. This trapped power is therefore greater than the power radiated in free space, by a factor greater than 10. This result, which shows the importance of trapped thermal radiation, is only marginally modified when the imaginary indices are reduced.

So far we have been interested in power transfer to modes at the design wavelength of the mirror ($\lambda = \lambda_0 = 2\mu$m). Note that due to the low uniform temperature of the component (20°C), thermal radiation is very low at this wavelength. We will now analyze the radiation trapped at

Optics EXPRESS

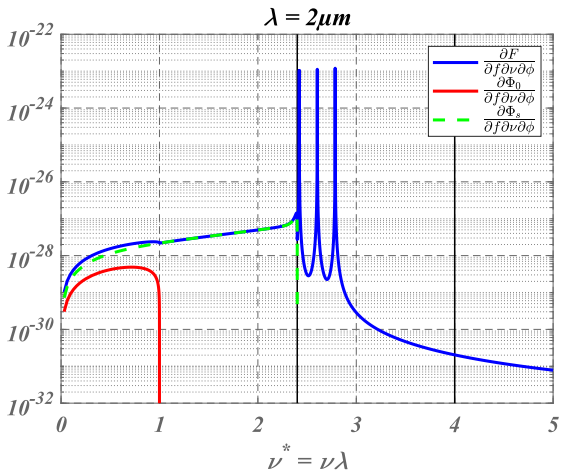

Fig. 5. Double power density supplied by thermal currents at $\lambda = \lambda_0 = 2\mu m$ for a 5-layer multi-dielectric mirror in TE polarization at thermal equilibrium (see text). The abscissa is the normalized spatial frequency given by $\nu^* = \lambda\nu$. The vertical bars indicate the separation between the different frequency windows (free space, modal, evanescent).

Table 2. Modes properties at $\lambda = \lambda_0 = 2\mu m$ of the 5 layer mirror of Fig.5. First line corresponds to the normalized spatial frequency of each mode. Second line shows the normalized spectral bandwidth around these modal frequencies. And finally, third line shows the power of thermal radiation transferred to each mode and normalized by the power of thermal radiation in free space.

	TE_0	TE_1	TE_2
Normalized spatial frequency $\nu_m^*=\nu_m\lambda_0$	2.7852	2.6036	2.4203
Spectral normalized bandwidth $\Delta\nu_m^*=\Delta\nu_m\lambda_0$	0.0015	0.0020	0.0022
Normalized power $P_g^m(\lambda_0)$	3.5899	4.3240	4.4028

longer mid-infrared wavelengths, i.e. $\lambda = 8\mu m$ where the signal power is at its maximum, as well as at an intermediate wavelength $\lambda = 4\mu m$. To do this, we first plot the power spectral density at $\lambda = 4\mu m$ in Fig. 6 a). The first thing to notice, as expected, is that the power density is much higher (about 5 decades) than that at $\lambda = 2\mu m$ (see Fig. 5). In addition, the number of modes is reduced, given the lower ratio e/λ of the total thickness e of the coating at wavelength $\lambda = 4\mu m$. A single mode is thus found at $\lambda = 4\mu m$, at the normalized frequency $\nu_m^* = 2.4794$. The power transmitted at this mode is 47.36% of the power radiated in free space over a normalized bandwidth of $9.46.10^{-4}$.

Finally, concerning the wavelength $\lambda = 8\mu m$, Fig. 6 b) shows that the structure no longer has any modes. In this case the energy dissipated in the modal window represents only $1.4\ 10^{-4}$ of that emerging in free space.

Optics EXPRESS

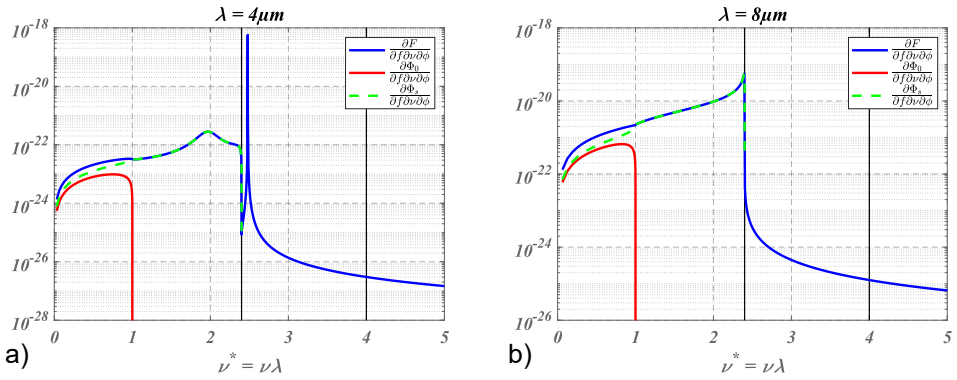

Fig. 6. Same legend than Fig. 5, but at wavelengths $\lambda = 4\mu m$ (left) and $\lambda = 8\mu m$ (right)

5. Conclusion

Much work has been devoted to the spectral and angular modification of thermal radiation by nanostructures such as diffraction gratings [27] or meta-surfaces [28], optical multilayers or photonic crystals [8,29,30]. Other work has focused on the decoupling of evanescent waves [12,31] in the vicinity of surfaces, resulting from thermal radiation. However, to our knowledge, this is the first time that trapped thermal radiation, transferred to the guided modes of a multilayer structure, has been modelled and calculated numerically.

We have presented a direct electromagnetic model based on the power supplied by the sources of thermal radiation given by the fluctuation-dissipation theorem [2,3]. The advantage of working with this quantity is that, unlike the Poynting flux, it gives access to the coupling efficiency of the energy transfer to the guided modes of the multilayer structure. This modelling is valid within the general framework of photo-induced absorption caused in the multilayer component by spatiotemporal illumination.

For the sake of simplicity, the numerical calculation was carried out at thermodynamic equilibrium, for a multi-dielectric mirror-type structure in the mid-infrared. It was thus possible to quantify precisely the energy transferred to each of the structure's modes. Generally speaking, the amount of radiation trapped in the modal window can be greater or less than that radiated into the free-space window, depending on the observation wavelength. We believe that these results could be very useful to the community, in particular by providing in-depth knowledge and understanding of loss budgets in precision systems affected by thermal radiation. It should also appeal to those involved in subsurface applications [32].

Acknowledgments. We acknowledge the joint laboratory (LabTop) which gathers CILAS and Institut Fresnel, for interesting discussions.

Disclosures. The authors declare no conflicts of interest.

Data availability. No data were generated or analyzed in the presented research.

References

1. J. R. Howell, M. P. Menguc, and R. Siegel, *Thermal Radiation Heat Transfer*, 6th ed. (CRC Press, 2015).
2. S. M. Rytov, I. A. Kravtsov, and V. I. Tatarskii, *Principles of Statistical Radiophysics. 3, Elements of Random Fields* (Springer, 1989).
3. L. Novotny and B. Hecht, *Principles of Nano-Optics*, 2nd ed. (Cambridge University Press, 2012).
4. Z. M. Zhang, *Nano/Microscale Heat Transfer*, 2nd edition, Mechanical Engineering Series (Springer, 2020).
5. C. Amra, M. Lequime, and M. Zerrad, *Electromagnetic Optics of Thin-Film Coatings: Light Scattering, Giant Field Enhancement, and Planar Microcavities* (Cambridge University Press, 2021).
6. H. A. Macleod, *Thin-Film Optical Filters* (CRC Press, 2021).

Optics EXPRESS

7. M. Francoeur, M. Pinar Mengüç, and R. Vaillon, "Solution of near-field thermal radiation in one-dimensional layered media using dyadic Green's functions and the scattering matrix method," J. Quant. Spectrosc. Radiat. Transf. **110**(18), 2002–2018 (2009).
8. L. P. Wang, S. Basu, and Z. M. Zhang, "Direct and indirect methods for calculating thermal emission from layered structures with nonuniform temperatures," J. Heat Transf. **133**(7), 072701 (2011).
9. D. L. C. Chan, M. Soljačić, and J. D. Joannopoulos, "Direct calculation of thermal emission for three-dimensionally periodic photonic crystal slabs," Phys. Rev. E **74**(3), 036615 (2006).
10. C. Luo, A. Narayanaswamy, G. Chen, *et al.*, "Thermal radiation from photonic crystals: a direct calculation," Phys. Rev. Lett. **93**(21), 213905 (2004).
11. J.-J. Greffet, P. Bouchon, G. Brucoli, *et al.*, "Light emission by nonequilibrium bodies: local Kirchhoff law," Phys. Rev. X **8**, 021008 (2018).
12. K. Joulain, J.-P. Mulet, F. Marquier, *et al.*, "Surface electromagnetic waves thermally excited: Radiative heat transfer, coherence properties and Casimir forces revisited in the near field," Surf. Sci. Rep. **57**(3-4), 59–112 (2005).
13. K. Joulain and A. Loizeau, "Coherent thermal emission by microstructured waveguides," J. Quant. Spectrosc. Radiat. Transf. **104**(2), 208–216 (2007).
14. P. Rouquette, C. Amra, M. Zerrad, *et al.*, "Photo-induced temperature in optical interference coatings," Opt. Express **30**(26), 46575 (2022).
15. C. Amra, D. Petiteau, M. Zerrad, *et al.*, "Analogies between optical propagation and heat diffusion: applications to microcavities, gratings and cloaks," Proc. R. Soc. Math. Phys. Eng. Sci. **471**, 20150143 (2015).
16. P. Rouquette, C. Amra, M. Zerrad, *et al.*, "Photo-induced thermal radiation of optical interference coatings submitted to a spatio-temporal illumination," Opt. Express **31**(22), 35431 (2023).
17. C. Amra and S. Maure, "Electromagnetic power provided by sources within multilayer optics: free-space and modal patterns," J. Opt. Soc. Am. A **14**(11), 3102 (1997).
18. C. Amra and S. Maure, "Mutual coherence and conical pattern of sources optimally excited within multilayer optics," J. Opt. Soc. Am. A **14**(11), 3114 (1997).
19. P. Baumeister, *Optical Coating Technology* (SPIE Optical Engineering Press, 2004).
20. F. Träger, ed., *Springer Handbook of Lasers and Optics: With 163 Tables*, 2. ed (Springer, 2012).
21. S. Volz and R. Carminati, *Microscale and Nanoscale Heat Transfer, Topics in Applied Physics* (Springer, 2007).
22. C. Amra, "First-order vector theory of bulk scattering in optical multilayers," J. Opt. Soc. Am. A **10**(2), 365 (1993).
23. A. Eroglu and J. K. Lee, "Simplified formulation of dyadic Green's functions and their duality relations for general anisotropic media," Prog. Electromagn. Res. **77**, 391–408 (2007).
24. C. Amra, M. Zerrad, and M. Lequime, "Trapped light scattering within optical coatings: a multilayer roughness-coupling process," Opt. Express **29**(16), 25570 (2021).
25. P. Rouquette, C. Amra, M. Zerrad, *et al.*, "Micro-cavity optimization for ultra-sensitive all-dielectric optical sensors," Opt. Express **30**(9), 15344 (2022).
26. "Crystran," https://www.crystran.co.uk/optical-materials.
27. J.-J. Greffet, R. Carminati, K. Joulain, *et al.*, "Coherent emission of light by thermal sources," Nature **416**(6876), 61–64 (2002).
28. X. Liu, T. Tyler, T. Starr, *et al.*, "Taming the blackbody with infrared metamaterials as selective thermal emitters," Phys. Rev. Lett. **107**(4), 045901 (2011).
29. B. J. Lee, C. J. Fu, and Z. M. Zhang, "Coherent thermal emission from one-dimensional photonic crystals," Appl. Phys. Lett. **87**(7), 071904 (2005).
30. B. J. Lee, Y.-B. Chen, and Z. M. Zhang, "Surface waves between metallic films and truncated photonic crystals observed with reflectance spectroscopy," Opt. Lett. **33**(3), 204 (2008).
31. K. Joulain, P. Ben-Abdallah, P.-O. Chapuis, *et al.*, "Strong tip–sample coupling in thermal radiation scanning tunneling microscopy," J. Quant. Spectrosc. Radiat. Transf. **136**, 1–15 (2014).
32. A. Farokh Payam and A. Passian, "Imaging beyond the surface region: Probing hidden materials via atomic force microscopy," Sci. Adv. **9**(26), eadg8292 (2023).